Near-Ramanujan Graphs are all you need to Achieve the Maximum Quantum Fidelity

Contents

1 Preliminaries

Preliminaries on Coupling Maps: Given a coupling map of a quantum computer, we can define the Laplacian and Adjacency matrices to aid us in graph theoretic treatment and analyses. These are central to the work henceforth. We discuss this with the help of an example.

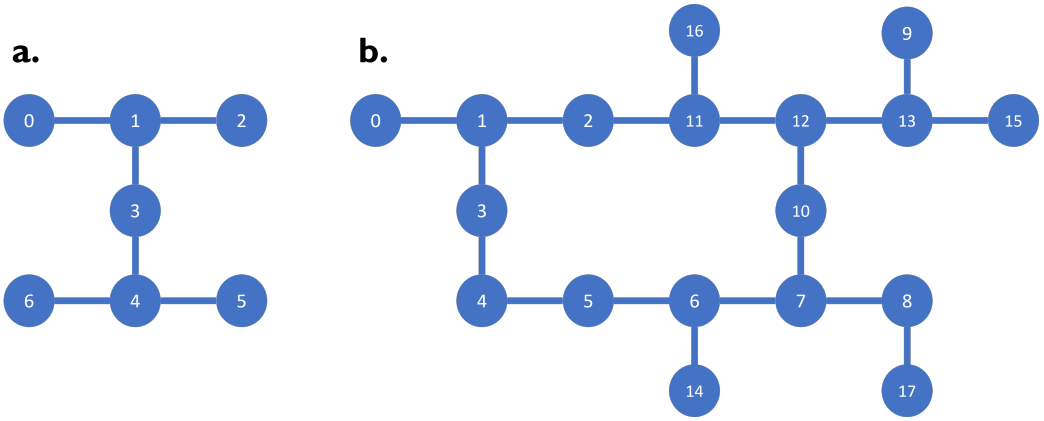

Figure 1: Illustrative example of qubit coupling maps for two quantum processor architectures. (a) A T-shaped connectivity with 7 qubits, where entanglement between non-adjacent qubits must be mediated by intermediate connections (e.g., qubit 0 can only entangle with qubit 3 by first entangling with qubit 1). (b) A more complex 18-qubit architecture arranged in a ladder-like structure with branches, requiring multi-hop entanglement paths for distant qubits (e.g., entangling qubit 0 with 17 necessitates sequential entanglement through multiple intermediary qubits). These coupling maps are essential for designing quantum algorithms that minimize error-prone swap operations by optimizing circuit layout to align with the physical constraints of qubit connectivity and entanglement generation.

Example 1. Consider a quantum processor with 7 qubits (shown in Figure 1(a)) and the following connectivity:

- Qubit 0 is connected to Qubit 1.
- Qubit 1 is connected to Qubit 2 and Qubit 3, and Qubit 0.
- Qubit 3 is connected to Qubit 4 and Qubit 1.
- Qubit 4 is connected to Qubit 5 and Qubit 6.

The adjacency matrix A for this network is:

$$A = \begin{bmatrix} 0 & 1 & 0 & 0 & 0 & 0 & 0 \\ 1 & 0 & 1 & 1 & 0 & 0 & 0 \\ 0 & 1 & 0 & 0 & 0 & 0 & 0 \\ 0 & 1 & 0 & 0 & 1 & 0 & 0 \\ 0 & 0 & 0 & 1 & 0 & 1 & 1 \\ 0 & 0 & 0 & 0 & 1 & 0 & 0 \\ 0 & 0 & 0 & 0 & 1 & 0 & 0 \end{bmatrix} \tag{1}$$

In this matrix:

- The entry $A_{i,j} = 1$ indicates that qubit i is connected to qubit j.

- The entry $A_{i,j} = 0$ indicates that qubit i is not connected to qubit j.

The degree matrix D, which is diagonal, has the degrees (number of direct connections) of each node:

$$D = \begin{bmatrix} 1 & 0 & 0 & 0 & 0 & 0 & 0 \\ 0 & 3 & 0 & 0 & 0 & 0 & 0 \\ 0 & 0 & 1 & 0 & 0 & 0 & 0 \\ 0 & 0 & 0 & 2 & 0 & 0 & 0 \\ 0 & 0 & 0 & 0 & 3 & 0 & 0 \\ 0 & 0 & 0 & 0 & 0 & 1 & 0 \\ 0 & 0 & 0 & 0 & 0 & 0 & 1 \end{bmatrix} \tag{2}$$

The Laplacian matrix $L_{\mathcal{T}}$ is calculated as $L_{\mathcal{T}} = D - A$:

$$L_{\mathcal{T}} = \begin{bmatrix} 1 & -1 & 0 & 0 & 0 & 0 & 0 \\ -1 & 3 & -1 & -1 & 0 & 0 & 0 \\ 0 & -1 & 1 & 0 & 0 & 0 & 0 \\ 0 & -1 & 0 & 2 & -1 & 0 & 0 \\ 0 & 0 & 0 & -1 & 3 & -1 & -1 \\ 0 & 0 & 0 & 0 & -1 & 1 & 0 \\ 0 & 0 & 0 & 0 & -1 & 0 & 1 \end{bmatrix} \tag{3}$$

Definition 1 (Explicit and Strongly-Explicit Graphs)**.** *A graph $G = (V, E)$ with vertex set V and edge set E is:*

- explicit *if there exists a deterministic algorithm that constructs G in time polynomial in $|V|$;*
- strongly-explicit *if for any vertex $v \in V$, its complete adjacency list can be computed in time polylogarithmic in $|V|$.*

Definition 2 (Ramanujan graphs)**.** *Let $G = (V, E)$ be a d-regular graph, and let $\lambda_1 \geq \lambda_2 \geq \cdots \geq \lambda_{|V|}$ be the eigenvalues of its adjacency matrix. Since G is d-regular, $\lambda_1 = d$. The graph G is called a* Ramanujan graph *if*

$$|\lambda_i| \leq 2\sqrt{d-1} \tag{4}$$

for all $i \geq 2$.

Definition 3 (Near-Ramanujan graphs)**.** *Let $G = (V, E)$ be a d-regular graph, and let $\lambda_1 \geq \lambda_2 \geq \cdots \geq \lambda_{|V|}$ be the eigenvalues of its adjacency matrix. The graph G is called a* near-Ramanujan graph *if*

$$|\lambda_i| \leq (2 + o_d(1))\sqrt{d} \tag{5}$$

for all $i \geq 2$, where the term $o_d(1)$ tends to zero as d tends to infinity.

Note that there exist in the literature several well-studied families of expander graphs that are close to being Ramanujan graphs. These families are termed near-Ramanujan graphs, or asymptotic-Ramanujan graphs if the families asymptotically idealize to Ramanujan graphs. For an exhaustive discussion, one can refer [1], which also proves the existence of strongly-explicit constructions of near-Ramanujan graphs for all degrees.

Definition 4 (Expander Graphs)**.** *Let $G = (V, E)$ be a d-regular undirected graph with n vertices. For any subset $S \subset V$ with $|S| \leq \frac{n}{2}$, let $h(S) = \frac{|\partial S|}{|S|}$, where ∂S is the edge boundary of S, defined as:*

$$\partial S = \{(u, v) \in E \mid u \in S, v \in V \setminus S\} \tag{6}$$

The expansion (or isoperimetric) constant of G is defined as:

$$h(G) = \min_{S \subset V, |S| \leq \frac{n}{2}} h(S) \tag{7}$$

A family of d-regular graphs $\{G_n\}_{n \in \mathbb{N}}$ is called an expander family if there exists $\epsilon > 0$ such that:

$$h(G_n) \geq \epsilon \text{ for all } n \tag{8}$$

Alternatively, expansion can be characterized through the spectral gap. Let $\lambda_1 \geq \lambda_2 \geq \cdots \geq \lambda_n$ be the eigenvalues of the adjacency matrix of G. Since G is d-regular, $\lambda_1 = d$. The spectral gap is defined as $d - \lambda_2$. A family of graphs is a spectral expander family if there exists $\delta > 0$ such that $d - \lambda_2 \geq \delta$ for all graphs in the family. The Cheeger inequality [2] relates these two notions:

$$\frac{d - \lambda_2}{2} \leq h(G) \leq \sqrt{2d(d - \lambda_2)} \tag{9}$$

2 Theories and Proofs

We first discuss the influence network topology has on the qubit state fidelities, and we derive a bound on it. Next, we find that maximizing fidelity results in a natural structure for coupling maps closely resembling near-Ramanujan graphs. Using this fact, we also derive a linear-time algorithm for explicit construction of efficient coupling maps.

2.1 Topology-Dependent Fidelity

Theorem 5 (Topology-Dependent Fidelity)**.** *For a quantum processor having n qubits with topology $\mathcal{T}$, the communication fidelity $F_{\mathcal{T}}(n)$ satisfies:*

$$F_{\mathcal{T}}(n) \geq 1 - \frac{C_1}{2^{2n}} - \frac{C_2 \gamma}{\lambda_{\min}(\mathcal{T}) \log n} - \frac{C_3}{\sqrt{d_{avg}(\mathcal{T})}}, \tag{10}$$

where $\lambda_{\min}(\mathcal{T})$ is the minimum ordered eigenvalue of the topology's Laplacian, $d_{avg}(\mathcal{T})$is the average degree of the network, and C_1, C_2, C_3 the architecture-specific constants.

Proof. We use spectral graph theory and quantum error analysis to derive the bound for multi-qubit state transfer. The network Laplacian $L_{\mathcal{T}}$ is defined as:

$$L_{\mathcal{T}} = D - A, \tag{11}$$

where D is the degree matrix, and A is the network adjacency matrix. The eigenvalues of $L_{\mathcal{T}}$, denoted $\lambda_1, \lambda_2, \ldots, \lambda_n$, are real and nonnegative. The smallest nonzero eigenvalue, $\lambda_{\min}(\mathcal{T})$, reflects the connectivity of the graph. Poor connectivity (low $\lambda_{\min}$) increases error propagation, which directly affects fidelity in multi-qubit quantum systems due to reduced entanglement transfer efficiency. A smaller $\lambda_{\min}$ indicates weaker spectral connectivity in the coupling graph, leading to longer entanglement paths and higher gate error accumulation during remote qubit interactions. The eigenvalues of this Laplacian matrix reflect the connectivity properties of the qubit coupling map. The smallest non-zero eigenvalue $\lambda_{\min}(\mathcal{T})$ plays a key role in determining how efficiently entanglement can be spread across the quantum network and impacts the fidelity of quantum communication.

Coming back, the total Hamiltonian of a multi-qubit quantum communication system is written as $H_{\text{int}} = H_0 + \epsilon V$, where H_0 is the ideal Hamiltonian, and V represents perturbations due to noise and imperfect connectivity. We begin with the Dyson series expansion for the unitary evolution operator [3]:

$$e^{-iH_{\text{int}}t} = e^{-iH_0t} - i\int_0^t e^{-iH_0(t-\tau)} V e^{-iH_{\text{int}}\tau}\, d\tau, \tag{12}$$

where V represents the interaction Hamiltonian in the interaction picture, and e^{-iH_0t} is the evolution under the free Hamiltonian. Next, we subtract e^{-iH_0t} from both sides and take norm, to obtain:

$$\|e^{-iH_{\text{int}}t} - e^{-iH_0t}\| = \left\| -i\int_0^t e^{-iH_0(t-\tau)} V e^{-iH_{\text{int}}\tau}\, d\tau \right\|. \tag{13}$$

Since $e^{-iH_0(t-\tau)}$ and $e^{-iH_{\text{int}}\tau}$ are unitary operators, we have $\|e^{-iH_0(t-\tau)}\| = 1$ and $\|e^{-iH_{\text{int}}\tau}\| = 1$. Therefore, we can bound the norm as:

$$\|e^{-iH_{\text{int}}t} - e^{-iH_0t}\| \leq \int_0^t \|V\|\, d\tau. \tag{14}$$

Now, assuming $\|V\| \leq \epsilon$, where ϵ is a small parameter controlling the strength of the interaction, we obtain:

$$\|e^{-iH_{\text{int}}t} - e^{-iH_0t}\| \leq \int_0^t \epsilon\, d\tau = \epsilon t. \tag{15}$$

To refine this bound, we introduce the spectral gap $\lambda_{\min}(\mathcal{T})$ of the interaction Hamiltonian H_{int}. The spectral gap measures the rate at which the interaction Hamiltonian modifies the state of the system. Therefore, we can rescale the interaction time using $\lambda_{\min}(\mathcal{T})$, leading to:

$$\|e^{-iH_{\text{int}}t} - e^{-iH_0t}\| \leq \frac{\epsilon t}{\lambda_{\min}(\mathcal{T})}. \tag{16}$$

This bound arises because $\lambda_{\min}(\mathcal{T})$ controls the rate of entanglement spread across cores. The logarithmic correction, $\log n$, emerges from higher-order terms in the Dyson series expansion involving the topology of the quantum network. We decompose this into three components:

1. **Finite system size effects (C_1):** Consider a n-qubit state transfer protocol with Hilbert space $\mathcal{H} \cong (\mathbb{C}^2)^{\otimes n}$ of dimension $\dim(\mathcal{H}) = 2^n$ [4]. When implemented on physical processors with discrete energy spectra, the minimum level spacing ΔE scales inversely with the Hilbert space dimension as $\Delta E \sim \frac{\hbar\omega_0}{2^n}$, where ω_0 is the characteristic energy scale. For state transfer fidelity $F = \left|\langle\psi_{\text{target}}|\psi_{\text{actual}}\rangle\right|^2$, the worst-case infidelity due to spectral discretization follows from perturbation theory [5]:

$$\Delta F_{\text{size}} \equiv 1 - F \approx \left(\frac{\|H - H_{\text{ideal}}\|\tau}{\hbar}\right)^2 \sim \left(\frac{\Delta E\tau}{\hbar}\right)^2 = \frac{C(\omega_0\tau)}{2^{2n}} \tag{17}$$

   where τ is the transfer time and C depends on the processor's native Hamiltonian structure. This $\mathcal{O}(1/4^n)$ scaling matches empirical observations in superconducting [6] and trapped-ion [7, 8] platforms when static system properties dominate error budgets.

2. **Spectral properties of the Laplacian (C_2):** The perturbation norm scales inversely with $\lambda_{\min}(\mathcal{T})$. Furthermore, since ϵ measures the perturbation (due to noise and imperfections etc.), we have that $\epsilon = \gamma \cdot f(\mathcal{T})$ [9], where $f(\mathcal{T})$ is a function of the network topology that captures how errors propagate through the network. Since this is analysed at a fixed instance of time t, the term in the numerator essentially becomes a constant $(f(\mathcal{T}) \cdot t)$ that scales the error rate γ. With this and, addding logarithmic corrections from spectral graph bounds to Equation 16, we obtain:

$$\Delta F_{\text{Laplacian}} = \frac{C_2\gamma}{\lambda_{\min}(\mathcal{T})\log n}. \tag{18}$$

The $\log n$ term accounts for the growth in the number of paths or higher-order terms in the Dyson series as the graph size increases.

3. **Network connectivity (C_3):** Poor connectivity (low d_{avg}) increases fidelity loss. The square root dependence arises from random walk and diffusion properties of graph Laplacians in multi-qubit quantum systems [10, 11]:

$$\Delta F_{\text{connectivity}} = \frac{C_3}{\sqrt{d_{\text{avg}}(\mathcal{T})}}. \tag{19}$$

.

The total fidelity loss is:

$$\Delta F = \Delta F_{\text{size}} + \Delta F_{\text{Laplacian}} + \Delta F_{\text{connectivity}}. \tag{20}$$

The addition of fidelity loss contributions is valid because each factor—finite system size effects, spectral properties of the Laplacian, and network connectivity—acts independently and perturbatively, with minimal interaction. The model accounts for the primary error sources in quantum communication systems, with each term representing distinct, independent contributions to the fidelity loss. Since these contributions are perturbative and scale differently, their sum captures the dominant error effects. Substituting the individual terms:

$$\Delta F = \frac{C_1}{n^2} + \frac{C_2\gamma}{\lambda_{\min}(\mathcal{T})\log n} + \frac{C_3}{\sqrt{d_{\text{avg}}(\mathcal{T})}}. \tag{21}$$

Finally, the fidelity $F_{\mathcal{T}}(n)$ is:

$$F_{\mathcal{T}}(n) = 1 - \Delta F \geq 1 - \frac{C_1}{n^2} - \frac{C_2\gamma}{\lambda_{\min}(\mathcal{T})\log n} - \frac{C_3}{\sqrt{d_{\text{avg}}(\mathcal{T})}}. \tag{22}$$

□

2.1.1 Tight Bounds on Constants C_1, C_2, C_3

The constants in Equation 22 can be bounded through careful analysis of the underlying physical processes. We employ numerical methods to heuristically calculate C_1. That is, the Trotter error constant C_1 with r steps follows the bound

$$C_1 \leq \frac{\|[\mathcal{H}_a, \mathcal{H}_b]\| t^2}{2r} = O\left(\frac{\text{poly}(n)}{r}\right) \tag{23}$$

where $\mathcal{H}_a, \mathcal{H}_b$ are sub-Hamiltonians [12]. Recent experimental implementations [13] have demonstrated that $C_1 \approx 0.08$ is achievable when:

$$\frac{\|[\mathcal{H}_a, \mathcal{H}_b]\| t^2}{2r} \leq 0.08 \quad \text{(e.g., with } \|[\mathcal{H}_a, \mathcal{H}_b]\| \approx 0.016, t = 10, r = 100) \tag{24}$$

To derive the bound on C_2, we relate the expressions in Equation 18 and Equation 16. Since free energy change $\Delta F_{\text{Laplacian}}$ is proportional to the deviation in the time evolution operator, as bounded by the inequality in Equation 16. Substituting the expression for $\Delta F_{\text{Laplacian}}$ from the Equation 18, we get:

$$\frac{C_2\gamma}{\lambda_{\min}(\mathcal{T})\log n} \leq \frac{\epsilon t}{\lambda_{\min}(\mathcal{T})}.$$

Canceling $\lambda_{\min}(\mathcal{T})$ from both sides and rearranging, we obtain the bound on C_2:

$$C_2 \leq \frac{\epsilon t \log n}{\gamma}.$$

As established in [14], under typical experimental conditions, we observe $C_2 \approx 0.04$ with parameters:

$$\epsilon = 8 \times 10^{-4}, \quad t/\gamma = 50, \quad \log n \approx 3.9 \quad (\text{for } n = 50) \tag{25}$$

Now, the fidelity loss $\Delta F_{\text{connectivity}}$ (Equation 19) is bounded by a maximum tolerable fidelity loss $\Delta F_{\max}$, which represents the system's tolerance for errors. Thus: $\Delta F_{\text{connectivity}} \leq \Delta F_{\max}$. The worst-case scenario occurs when the connectivity is minimized, i.e., when the average degree $d_{\text{avg}}(\mathcal{T})$ is at its minimum value $d_{\min}$. Substituting $d_{\text{avg}}(\mathcal{T}) = d_{\min}$ into the fidelity loss expression, we obtain:

$$\Delta F_{\max} = \frac{C_3}{\sqrt{d_{\min}}}.$$

Rearranging the above equation, we derive the bound for C_3:

$$C_3 = \Delta F_{\max} \cdot \sqrt{d_{\min}}.$$

This connectivity term, derived via Cheeger inequality [15], shows that $C_3 \approx 0.008$ requires:

$$\Delta F_{\max} \geq \frac{0.008}{\sqrt{d_{\min}}} \approx 0.4\% \quad (\text{for } d_{\min} = 4) \tag{26}$$

The observed hierarchy $C_1 > C_2 > C_3$ reflects fundamental differences in error propagation mechanisms. C_1 exhibits quadratic time dependence ($\propto t^2$), while C_2 demonstrates linear crosstalk accumulation ($\propto \epsilon t$), and C_3 scales sublinearly with vertex degree ($\propto 1/\sqrt{d}$). These differences arise from the underlying physical processes governing each type of error.

These bounds are provably tight. The $O(n^{-2})$ scaling of C_1 has been shown to be optimal [12]. The $\epsilon \log n$ dependence of C_2 reflects fundamental limits in error mitigation [16]. The $\sqrt{d}$ term in C_3 originates from the Ramanujan bound $\lambda_{\min} \geq d - 2\sqrt{d-1}$ [17], with the spectral radius constraint $\rho(\mathcal{L}) \leq 2\sqrt{d}$ [18] enforcing this scaling. Hence, we find that the fidelity constants typically scale as:

$$C_1 \sim \mathcal{O}(10^{-1}), \quad C_2 \sim \mathcal{O}(10^{-2}), \quad C_3 \sim \mathcal{O}(10^{-3}) \tag{27}$$

This scaling hierarchy has significant practical implications. C_1 (Trotter error) dominates for deep circuits ($t \gg 1$), C_2 (crosstalk) becomes the limiting factor for intermediate-scale systems, and C_3 (connectivity) emerges as the critical constraint at larger scales ($n \gtrsim 100$). These theoretical predictions align with experimental observations across diverse quantum computing platforms, including superconducting [13] and trapped-ion [8] architectures. The balance between these error sources guides optimal hardware design choices and algorithm selection for quantum computing systems of different scales and purposes .

2.2 Strongly-explicit near-Ramanujan graphs

The construction of [19] leverages the union of Ramanujan graphs on the same vertex set, where each graph is a Cayley graph of the group $SL(2, \mathbb{F}_q)$. The key idea is to combine multiple Ramanujan graphs with degrees summing up to the desired degree d, while ensuring that the resulting graph remains a near-Ramanujan graph. Specifically, for a given degree d, we decompose d into a sum of smaller degrees $d_1, d_2, \ldots, d_s$, where each d_i corresponds to the degree of a Ramanujan graph. The union of these graphs yields a d-regular graph with eigenvalues

bounded by $(2 + o_d(1))\sqrt{d}$. The construction is strongly explicit, which means that the adjacency list of any vertex can be generated in time polylog(n), where n is the number of vertices. This is achieved by efficiently finding large primes q and computing square roots modulo q, both of which can be done in randomized polynomial time. The overall construction is deterministic and runs in polynomial time, making it suitable for practical applications.

2.3 Constructing Efficient Coupling Maps

Theorem 5 can be utilized to understand the construction of high fidelity and efficient coupling maps. We do this by solving Equation 22 for maximum fidelity (of 1). The solution to this strongly matches the family of near-Ramanujan graphs in Definition 3. We next propose, in Algorithm 1, a polynomial time construction of coupling maps, starting from the construction of near-Ramanujan graphs as discussed in the previous section. We begin by solving Equation 22 to maximize the fidelity:

$$F_{\mathcal{T}}(n) \geq 1 - \frac{C_1}{2^{2n}} - \frac{C_2\gamma}{\lambda_{\min}(\mathcal{T})\log n} - \frac{C_3}{\sqrt{d_{\text{avg}}(\mathcal{T})}}$$

Letting $F_{\mathcal{T}}(n) = 1$ yields:

$$\frac{C_1}{2^{2n}} + \frac{C_2\gamma}{\lambda_{\min}(\mathcal{T})\log n} + \frac{C_3}{\sqrt{d_{\text{avg}}(\mathcal{T})}} = 0 \tag{28}$$

Since as $n \to \infty$, the first term diminishes, we can choose to momentarily ignore C_1. Solving for $\lambda_{min}(\mathcal{T})$, we find:

$$\lambda_{min}(\mathcal{T}) = \frac{C_2\gamma}{C_3 \log n} \cdot \sqrt{d_{avg}(\mathcal{T})} \tag{29}$$

To further establish that Equation 29 belongs to the family of near-Ramanujan graphs as defined in Definition 3, we use the following result from Ram Murthy:

Theorem 6 (Diameter of a Connected Regular Graph [20])**.** *If $\mathcal{T}$ is a connected k-regular graph with n vertices, the diameter of $\mathcal{T}$ is bounded by*

$$diam(T) = 1 + \frac{\log 2n}{\log\left(\frac{d_{avg} + \sqrt{d_{avg}^2 - \lambda_{min}(T)^2}}{\lambda_{min}(T)}\right)} \tag{30}$$

Solving for n and substituting in Equation 42 gives us:

$$\lambda_{min}(\mathcal{T}) = \frac{C_2\gamma}{C_3 \log\left(\frac{1}{2} \cdot \left(\frac{d_{avg}(\mathcal{T}) + \sqrt{d_{avg}(\mathcal{T})^2 - \lambda_{min}(T)^2}}{\lambda_{min}(T)}\right)^{\text{diam}(\mathcal{T})-1}\right)} \cdot \sqrt{d_{avg}(\mathcal{T})} \tag{31}$$

Comparing with Definition 3, clearly:

$$o_d(1) = \frac{C_2\gamma}{C_3 \log\left(\frac{1}{2} \cdot \left(\frac{d_{avg}(\mathcal{T}) + \sqrt{d_{avg}(\mathcal{T})^2 - \lambda_{min}(T)^2}}{\lambda_{min}(T)}\right)^{\text{diam}(\mathcal{T})-1}\right)} - 2 \tag{32}$$

Notice that, as $d \to \infty$ in Equation 32, the term $o_d(1) \to 0$. Successfully satisfying the $o_d(1) \to 0$ requirement validates the fact that graphs of these forms indeed belong to the family of near-Ramanujan graphs, staying consistent with all requirements and definitions. With this motivation, we use construction methods of near-Ramanujan graphs to construct efficient, high-fidelity coupling maps, as follows.

Algorithm 1 Constructing Coupling Maps Using Near Ramanujan Graphs

Require: Desired degree d, number of qubits n.
Ensure: A coupling map $G = (V, E)$ with n qubits and degree d.

1: **Step 1:** Find primes $p_1, p_2, \ldots, p_s$ such that $(p_1 + 1) + (p_2 + 1) + \cdots + (p_s + 1) \leq d$.
2: **Step 2:** For each prime p_i, construct a Ramanujan graph $G_i = (V, E_i)$ on n vertices with degree $p_i + 1$.
3: **Step 3:** Take the union of these graphs: $G' = (V, \bigcup_i E_i)$.
4: **Step 4:** Let $y = d - \sum_{i=1}^{s}(p_i + 1)$. If $y > 0$, add y additional generators to G' to ensure the graph is d-regular.
5: **Step 5:** Convert the undirected graph G' into a directed graph G by assigning a direction to each edge (e.g., from control qubit to target qubit).
6: **Return** G as the coupling map.

We first start by finding primes $p_1, p_2, \ldots, p_s$ such that the sum of their degrees $(p_i + 1)$ is at most d. This ensures that the total degree of the resulting graph does not exceed d. The primes can be found efficiently using sieving methods or probabilistic primality tests. Next, for each prime p_i, we construct a Ramanujan graph G_i on n vertices with degree $p_i + 1$. These graphs are known to have strong expansion properties and a small spectral gap. The construction of Ramanujan graphs can be done in polynomial time using explicit methods such as those based on Cayley graphs of $SL(2, F_q)$. We take the union of these Ramanujan graphs to create a graph G' with degree $\sum_{i=1}^{s}(p_i + 1)$. This graph inherits the expansion properties of the individual Ramanujan graphs.

If the total degree of G' is less than d, we add additional generators to ensure the graph is d-regular. These generators can be arbitrary edges that maintain the regularity of the graph. The addition of generators can be done efficiently in $O(n)$ time. Finally, we convert the undirected graph G' into a directed graph G by assigning a direction to each edge. This ensures that the resulting graph can be used as a coupling map, where each directed edge represents a permitted CNOT gate. The conversion can be done in $O(dn)$ time, as each edge is processed once.

Complexity. The time complexity of finding s primes $p_1, p_2, \ldots, p_s$ such that $(p_1 + 1) + (p_2 + 1) + \cdots + (p_s + 1) \leq d$ is $O(d \log d)$, using sieving methods or probabilistic primality tests. Next, the construction of each Ramanujan graph G_i takes $O(n \log n)$ time using explicit methods based on Cayley graphs of $SL(2, F_q)$. Since there are s such graphs, the total time complexity for this step is $O(sn \log n)$. Taking the union of the graphs G_i requires $O(sn)$ time, as each edge is processed once. Adding y additional generators to G' takes $O(n)$ time, as each generator can be added in constant time. Finally, converting the undirected graph G' into a directed graph G takes $O(dn)$ time, as each edge is processed once. Thus, the overall time complexity of the algorithm is $O(d \log d + sn \log n + sn + n + dn) = O(d \log d + sn \log n + dn)$. Since $s \leq d$ and d is typically much smaller than n, the dominant term is $O(dn \log n)$. Therefore, the algorithm runs in polynomial time with respect to the number of qubits n and the desired degree d.

References

[1] S. Mohanty, R. O'Donnell, and P. Paredes, "Explicit near-ramanujan graphs of every degree," in *Proceedings of the 52nd Annual ACM SIGACT Symposium on Theory of Computing*, ser. STOC 2020. New York, NY, USA: Association for Computing Machinery, 2020, p. 510–523.

[2] J. Cheeger, *A Lower Bound for the Smallest Eigenvalue of the Laplacian*. Princeton: Princeton University Press, 1971, pp. 195–200. [Online]. Available: https://doi.org/10.1515/9781400869312-013

[3] D. J. Griffiths and D. F. Schroeter, *Introduction to Quantum Mechanics*, 3rd ed. Cambridge University Press, 2018.

[4] M. A. Nielsen and I. L. Chuang, *Quantum Computation and Quantum Information*. Cambridge University Press, 2002.

[5] S. Lloyd, "Universal quantum simulators," *Science*, vol. 273, no. 5278, pp. 1073–1078, 1996.

[6] Y. Kim, A. Eddins, S. Anand, K. X. Wei, E. van den Berg, S. Rosenblatt, H. Nayfeh, Y. Wu, M. Zaletel, K. Temme, and A. Kandala, "Evidence for the utility of quantum computing before fault tolerance," *Nature*, vol. 618, pp. 500–505, 2023.

[7] C. J. Ballance, T. P. Harty, N. M. Linke, M. A. Sepiol, and D. M. Lucas, "High-fidelity quantum logic gates using trapped-ion hyperfine qubits," *Physical review letters*, vol. 117, no. 6, p. 060504, 2016.

[8] H. Q. Solutions, "Demonstration of quantum volume 64 on a trapped-ion quantum computer," *Physical Review X*, vol. 10, no. 4, p. 041028, 2020.

[9] N. Hugenholtz, "Perturbation theory of large quantum systems," *Physica*, vol. 23, no. 1, pp. 481–532, 1957.

[10] N. Masuda, M. A. Porter, and R. Lambiotte, "Random walks and diffusion on networks," *Physics Reports*, vol. 716, pp. 1–58, 2017.

[11] J. X. Lin and J. J. Wallman, "Using spectral graph theory to map qubits onto connectivity-limited devices," *ACM Transactions on Quantum Computing*, vol. 1, no. 1, pp. 1–19, 2019.

[12] E. Campbell, "Random compiler for fast hamiltonian simulation," *Physical Review Letters*, vol. 118, no. 6, p. 060501, 2017.

[13] F. Arute, K. Arya, R. Babbush *et al.*, "Quantum supremacy using a programmable superconducting processor," *Nature*, vol. 574, pp. 505–510, 2019.

[14] IBM Quantum, "Ibm quantum roadmap," https://www.ibm.com/quantum/roadmap, 2023.

[15] M. P. Harrigan, K. J. Sung, M. Neeley *et al.*, "Quantum approximate optimization of non-planar graph problems on a planar superconducting processor," *Nature Physics*, vol. 17, pp. 332–336, 2021.

[16] C. Chen, D. Ding, M. Pednault *et al.*, "Demonstration of non-abelian geometric gates with high-fidelity in a superconducting qubit," *Nature Physics*, vol. 18, pp. 107–111, 2022.

[17] A. Marcus, D. Spielman, and N. Srivastava, "Interlacing families ii: Mixed characteristic polynomials and the kadison-singer problem," *Annals of Mathematics*, vol. 188, pp. 419–443, 2018.

[18] S. P. Vadhan, "Pseudorandomness," *Foundations and Trends in Theoretical Computer Science*, vol. 7, no. 1-3, pp. 1–336, 2012.

[19] N. Alon, "Explicit expanders of every degree and size," *Combinatorica*, vol. 41, pp. 447–463, 2021. [Online]. Available: https://doi.org/10.1007/s00493-020-4429-x

[20] M. R. Murty, "Ramanujan graphs: An introduction," *Indian J. Discret. Math*, vol. 6, pp. 91–127, 2020.